AMERICAN SOCIETY FOR MICROBIOLOGY | mBio®

RESEARCH ARTICLE

Glucose-1,6-Bisphosphate, a Key Metabolic Regulator, Is Synthesized by a Distinct Family of α-Phosphohexomutases Widely Distributed in Prokaryotes

Niels Neumann,[a,b] Simon Friz,[a,b] Karl Forchhammer[a,b]

[a]Interfaculty Institute of Microbiology and Infection Medicine, University of Tübingen, Tübingen, Germany
[b]Cluster of Excellence: EXC 2124: Controlling Microbes to Fight Infection, Tübingen, Germany

ABSTRACT The reactions of α-d-phosphohexomutases (αPHM) are ubiquitous, key to primary metabolism, and essential for several processes in all domains of life. The functionality of these enzymes relies on an initial phosphorylation step which requires the presence of α-d-glucose-1,6-bisphosphate (Glc-1,6-BP). While well investigated in vertebrates, the origin of this activator compound in bacteria is unknown. Here we show that the Slr1334 protein from the unicellular cyanobacterium *Synechocysitis* sp. PCC 6803 is a Glc-1,6-BP-synthase. Biochemical analysis revealed that Slr1334 efficiently converts fructose-1,6-bisphosphate (Frc-1,6-BP) and α-d-glucose-1-phosphate/α-d-glucose-6-phosphate into Glc-1,6-BP and also catalyzes the reverse reaction. As inferred from phylogenetic analysis, the *slr1334* product belongs to a primordial subfamily of αPHMs that is present especially in deeply branching bacteria and also includes human commensals and pathogens. Remarkably, the homologue of Slr1334 in the human gut bacterium *Bacteroides salyersiae* catalyzes the same reaction, suggesting a conserved and essential role for the members of this αPHM subfamily.

IMPORTANCE Glc-1,6-BP is known as an essential activator of phosphoglucomutase (PGM) and other members of the αPHM superfamily, making it a central regulator in glycogen metabolism, glycolysis, amino sugar formation as well as bacterial cell wall and capsule formation. Despite this essential role in carbon metabolism, its origin in prokaryotes has so far remained elusive. In this study we identify a member of a specific αPHM subfamily as the first bacterial Glc-1,6-BP synthase, forming free Glc-1,6-BP by using Frc-1,6-BP as phosphoryl-donor. PGMs of this subfamily are widely distributed among prokaryotes including human commensals and pathogens. By showing that a distinct subfamily member can also form Glc-1,6-BP, we provide evidence that Glc-1,6-BP synthase activity is a general feature of this group.

KEYWORDS carbon metabolism, glucose-1,6-bisphosphate, glycolysis, phosphoglucomutase

The α-d-phosphohexomutase (αPHM) superfamily is ubiquitous and found in all domains of life. All known members of this superfamily catalyze a reversible intramolecular phosphoryl transfer on their phosphosugar substrates. This reaction requires a bound metal ion (usually Mg^{2+}) together with a conserved phosphorylated seryl residue in the active site and proceeds via a bis-phosphorylated sugar intermediate (1). While showing similar properties in structure and reaction mechanism, these enzymes differ strongly in substrate specificity. Based on their preferred substrate, the αPHMs are traditionally divided into four main groups: (i) Phosphoglucomutases (PGM), (ii) phosphoglucosamine mutases (PNGM), (iii) phosphoacetylglucosamine mutases (PAGM), and (iv) the group of bifunctional phosphoglucomutases/phosphomannomutases (PGM/PMM) (1). The most recent expansion to this classification has been the discovery of the mammalian phosphopentomutase (PGM2) and

Editor Eleftherios T. Papoutsakis, University of Delaware

Address correspondence to Karl Forchhammer, karl.forchhammer@uni-tuebingen.de.

The authors declare no conflict of interest.

Received 2 June 2022
Accepted 5 July 2022
Published 20 July 2022

TABLE 1 Subfamilies in the αPHM superfamily with their identifier and proposed main function according to the NCBI conserved domain database (CDD)

CDD group name	CDD identifier	Proposed main function
PGM1	cd03085	Phosphoglucomutase
PGM2	cd05799	Phosphopentomutase (PGM2)/Glc-1,6-BP synthase (PGM2L1)
PGM3(PAGM)	cd03086	Phosphoacetylglucosamine mutase
PMM/PGM	cd03089	Bi-functional phosphomanno-/phosphoglucomutase
PGM like 1	cd03087	Unknown
PGM like 2	cd05800	Unknown
PGM like 3	cd05801	Phosphoglucomutase
PGM like 4	cd05803	Unknown
ManB	cd03088	Phosphomannomutase
GlmM	cd05802	Phosphoglucosamine mutase

glucose-1,6-bisphosphate-synthase (PGM2L1) (2, 3). This classification, however, lacks a more detailed subdivision in between the main groups and also does not take into account αPHMs preferably catalyzing other reactions (e.g., straight phosphomannomutases) (3). The NCBI conserved domain database (CDD), instead, classifies the αPHM superfamily in 11 different subfamilies on a phylogenetic basis (4). This phylogenetic model enables a more detailed classification and includes several groups of bacterial and archaeal enzymes showing typical αPHM properties but being only poorly characterized (Table 1).

The PGM (cd03085) from rabbit and human as well as the bacterial PGM (cd05801) from *Salmonella typhimurium* and the bacterial bifunctional PMM/PGM (cd03089) from *Pseudomonas aeruginosa* are among the best characterized αPHMs with available crystal structures and detailed description of reaction mechanisms (5–9). Catalyzing the interconversion of α-d-glucose-1P (Glc-1P) and α-d-glucose-6P (Glc-6P) makes PGM a key enzyme in glycogen metabolism, glycolysis, and gluconeogenesis. During this reaction, a phosphoserine at the active site of PGM donates the phosphoryl group to the substrate Glc-6P or Glc-1P resulting in the synthesis of the transient intermediate α-d-glucose-1,6-bisphosphate (Glc-1,6-BP). After a reorientation in the catalytic center, the intermediate product re-phosphorylates the active site serine yielding Glc-1P or Glc-6P, respectively. Glc-1,6-BP itself acts as an essential activator of PGM by providing an initial phosphorylation of the active site and was first discovered by Leloir, Trucco (10) in yeast extract (11). While Glc-1,6-BP is not a free metabolite in any metabolic pathway, it is known to be a potent regulator of several enzymes in central carbon metabolism in eukaryotes: in addition to PGMs and other αPHMs, it was shown to regulate hexokinases, 6-phosphogluconate dehydrogenase, phosphofructokinase and pyruvate kinase (12). In mammalian tissues the majority of Glc-1,6-BP is catalyzed by the PGM2L1 enzyme, a member of the cd05799 subfamily exclusive to eukaryotes, utilizing 1,3-bisphosphoglyceric acid (1,3-BPG) as phosphoryl donor for Glc-1P (3). In contrast, despite its essential role in the activity of prokaryotic PGM and other enzymes, the origin of Glc-1,6-BP in prokaryotes has been overlooked and no enzyme producing free Glc-1,6-BP has been identified so far (13, 14).

The unicellular cyanobacterium *Synechocystis* sp. PCC 6803 (hereafter *Synechocystis*) expresses two enzymes that are encoded by the genes *sll0726* and *slr1334* and annotated as PGM-like (4, 15). While Sll0726 exhibits typical properties of PGMs (16–18), little is known about Slr1334. The only study addressing this issue reported that purified *Synechocystis* Sll0726 has about a 10-fold higher activity *in vitro* than Slr1334 and that a *sll0726* knockout mutant only shows around 3% PGM activity compared to the wild-type (19). Despite its low contribution to overall PGM activity, the Slr1334 product appeared to be essential as it was not possible to acquire fully segregated knockout mutants of the *slr1334* gene, which raised the question of the role of Slr1334 in *Synechocystis*.

In this work, we show that Slr1334 has a phosphotransferase activity catalyzing the production of free Glc-1,6-BP from Glc-1P/Glc-6P and fructose-1,6-bisphosphate (Frc-1,6-BP). Thereby, Slr1334 is responsible for the formation of the key activator of PGM,

Glc-1,6-BP, making it a major regulator in glycolysis and other carbon pathways. Our finding makes Slr1334 the first bacterial enzyme specific for the production of free Glc-1,6-BP. Importantly, we show that the homologue of Slr1334 in the human gut bacterium *Bacteroides salyersiae* catalyzes the same reaction.

RESULTS

Classification of the two PGM isoenzymes from *Synechocystis*. *Synechocystis* possesses two genes annotated as PGMs, the genes *sll0726* and *slr1334*. To classify them within the αPHM superfamily, we performed a phylogenetic analysis by multi-level alignment of all αPHM subfamilies that are considered PGM or "PGM_like." For this, we collected the entry sequences from the NCBI Conserved Domains Database (CDD) (4) and retrieved further sequences by performing BLAST searches in the NCBI RefSeq_protein database. To focus on glucose-specific αPHMs, the groups of enzymes specific for other sugars like PMMs, PNGM and PAGMs (cd03086 cd03088, cd05802, cd05805) were omitted from the analysis (Fig. 1). In general, the αPHMs can be divided into four conserved regions which are from N- to C-terminus: (i) the active site domain, (ii) the metal binding domain, (iii) the sugar binding, and (iv) the phosphate binding domain. While the domains 1, 2, and 4 are usually highly conserved between the different subfamilies, the sugar binding domain shows a greater variance and can assist in the categorization of αPHMs (Table S1 in the supplemental material) (2).

Slr1334 is part of the cd05800 (PGM_like2) subfamily present in many bacterial groups. In agreement with the CDD, our phylogenetic analysis shows that this subfamily forms a distinct cluster of PGMs which clearly separates from other PGM and PGM like enzymes. The Sll0726 PGM, by contrast, is a member of the cd05801 subfamily, to which the well characterized PGM from *S. typhimurium* belongs. With the chosen parameters (see methods part) we detected a total of 2140 hits for Slr1334 homologues.

Slr1334 shows low PGM activity compared to Sll0726 but behaves differently in the presence of fructose-1,6-BP. To gain deeper insights into the role of the enigmatic Slr1334, we overexpressed Sll0726 along with Slr1334 in *Escherichia coli* and assessed the PGM enzymatic activity of the purified proteins by measuring the interconversion of Glc-1-P to Glc-6-P in an assay that couples Glc-6-P formation to its subsequent oxidation using glucose-6-phosphate-dehydrogenase (G6PDH) and $NADP^+$. We could show that Slr1334 only displays about 5% of catalytic efficiency compared to Sll0726 when both PGMs were tested with saturating amounts of the activator Glc-1,6-BP (60 μM) (Fig. 2, Table 2; see also Fig. 3). Interestingly, the PGM activity of both enzymes was also measurable without addition of Glc-1,6-BP, which is considered to be an essential activator. However, in the absence of Glc-1,6-BP, the catalytic efficiency was about 70 times lower due to a significantly increased Michaelis-Menten constant (K_m) for Sll0726 and Slr1334 alike.

Fructose-1,6- bisphosphate is an endogenous intermediate of the glycolytic pathway and is known to be an inhibitor of PGM most likely by competing with the reaction intermediate Glc-1,6-BP (20, 21). In a preliminary experiment we tested the effect of different concentrations of Frc-1,6-BP on Sll0726 and observed major inhibition already at concentrations of 100 μM (data not shown). When testing PGM activity by replacing 60 μM Glc-1,6-BP with 100 μM Frc-1,6-BP, we detected a decrease in catalytic efficiency to 19% as a consequence of a strongly increased K_m (Fig. 2, Table 2). Strikingly, however, for Slr1334 we detected a different effect: while the catalytic rate constant (k_{cat}) decreased by about 2-fold, we measured an approximately 100-fold reduced K_m resulting in 50 times increased catalytic efficiency. This raised the question of how Frc-1,6-BP affected the PGM-activity of Slr1334. We speculated that Frc-1,6-BP might either function as a direct activator similar to Glc-1,6-BP or be required for the synthesis of the activating compound Glc-1,6-BP during the reaction of Slr1334. As we will show below, the activating compound turned out to be Glc-1,6-BP and not Frc-1,6-BP.

Slr1334 forms a product out of Frc-1,6-BP and Glc-1P/Glc-6P that strongly activates PGM reaction of Sll0726. To determine the amount of Glc-1,6-BP needed to achieve activation of the Sll0726 PGM reaction at 1 mM Glc-1P we first tested PGM activity

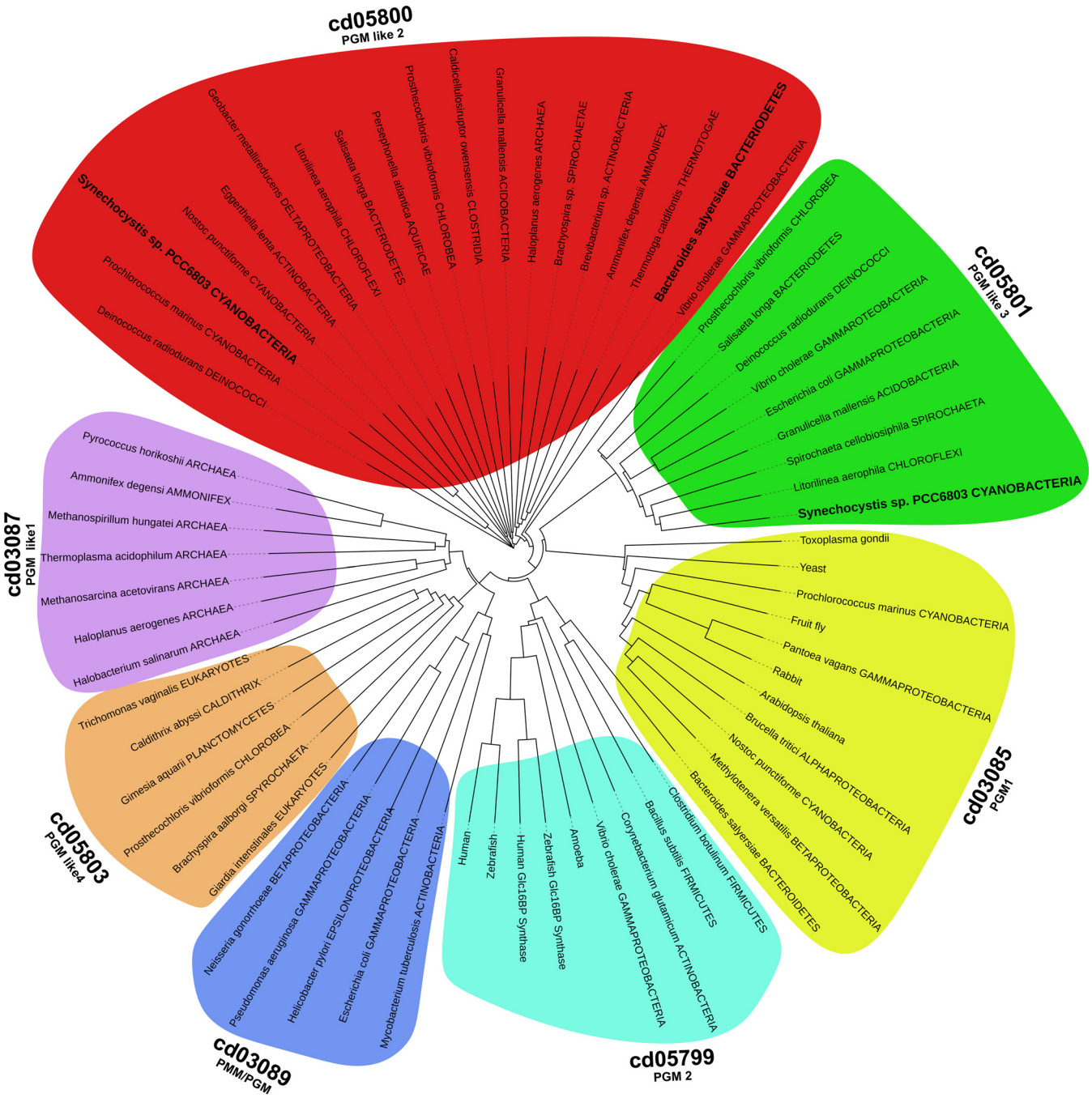

FIG 1 Phylogenetic tree of the αPHM subfamilies that are considered to be "PGM-like" according to CDD. The tree was built on the taxonomy based on the protein sequences present in the NCBI RefSeq_protein database. The CDD subfamilies cd03086, cd03088, cd05802 and cd05805, which are known to catalyze distinct reactions, were omitted from the analysis. The organisms investigated in this study are highlighted in bold letters.

of Sll0726 at different Glc-1,6-BP concentrations. Maximum activation was achieved at Glc-1,6-BP concentrations between 30 and 60 μM resulting in a 5-fold increased activity compared to a control reaction without any effectors (Fig. 3). Next, we incubated Slr1334 (0.5 μM) with the phosphorylated sugars Frc-1,6-BP, Glc-1P and Glc-6P (1 mM each) in different combinations and subsequently tested whether the Sll0726 PGM reaction could be activated by the corresponding reaction products (Fig. 3). As a control, we incubated the same phosphosugars with Sll0726 (0.5 μM) instead of Slr1334 before testing activation of the Sll0726 PGM reaction. After incubating Slr1334 and the control reaction with the phosphosugars for 1.5 h, the reaction was stopped by heat inactivation and the supernatant was added in a dilution of 1:10 to the reaction mixture of the Sll0726 PGM reaction assay,

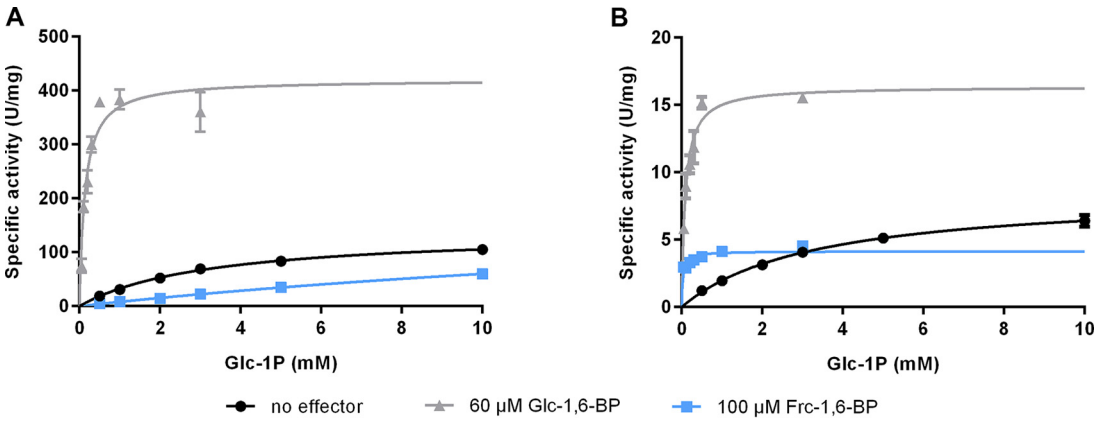

FIG 2 Slr1334 shows lower PGM activity then Sll0726 and behaves differently in the presence of Frc-1,6-BP. Shown are the Michaelis-Menten kinetics of Sll0726 (A) and Slr1334 (B): in black, without addition of effectors; in light gray in the presence of 60 μM Glc-1,6-BP; in blue, in the presence of 100 μM Frc-1,6-BP. Three replicates were measured for each data-point. Error bars represent the SD.

which was then started by adding 1 mM Glc-1P. Only after adding the supernatant of the Slr1334 reaction containing Frc-1,6-BP and Glc-1P (or Glc-6P) as substrates, the velocity of the Sll0726 PGM reaction was increased by 5-fold in comparison to the control reaction without any effector (Fig. 3). When the Sll0726 PGM reaction was performed with the supernatant of the Sll0726 control reaction or the reaction products of Slr1334 using Frc-1,6-BP as sole substrate, the enzyme velocity was lower than the control without effectors. This reduction can be explained by the inhibitory effect of Frc-1,6-BP on Sll0726 as shown in Fig. 2.

In addition to Frc-1,6-BP, we also tested whether Slr1334 can utilize 1,3-BPG instead of Frc-1,6-BP for Glc-1,6-BP formation as described for the mammalian PGM2L1. Since 1,3-BPG is not commercially available, we established an assay whereby we continuously produced 1,3-BPG by a phosphoglycerate kinase (PGK) reaction using a His-tagged purified PGK in combination with 1 mM 3PG and 1 mM ATP (see methods part). This reaction was directly coupled to the reaction of Slr1334 with Glc-1P or Glc-6P or no substrate. As a control the same reaction was performed with Sll0726 instead of Slr1334. To test the possible formation of Glc-1,6-BP, the supernatants of these reactions were added to the Sll0726 PGM reaction before performing the enzymatic assay as described above.

We detected an increase in the Sll0726 PGM activity by approximately 2.5-fold compared to the control without effectors when the supernatant of the Slr1334 reaction contained 1,3-BPG and either Glc-1P or Glc-6P. No increase in activity was detected when the supernatant solely contained 1,3-BPG. The supernatant of the control reaction with Sll0726 instead of Slr1334 resulted in no marked change in activity.

By comparing the activation of the Sll0726 PGM reaction by the Slr1334 reaction products to the activation at different concentration of Glc-1,6-BP we attempted to estimate the efficiency of Glc-1,6-BP formation from either Frc-1,6-BP or 1,3-BPG. In this experiment, the Slr1334-catalyzed reaction using 1,3-BPG and G1P as substrates produced an estimated 1–5 μM the activating compound, while the F-1,6-BP + G1P

TABLE 2 Kinetic parameters for the conversion of Glc-1P to Glc-6P by Sll0726 and Slr1334 in the presence of different effector molecules as indicated[a]

	Sll0726			Slr1334			Catalytic efficiency ratio (%)
Effector	K_m (mM)	K_{cat} (s^{-1})	K_{cat}/K_m ($M^{-1}s^{-1}$)	K_m (mM)	K_{cat} (s^{-1})	K_{cat}/K_m ($M^{-1}s^{-1}$)	(Slr1334/Sll0726)
No effector	3.27 ± 0.21	138 ± 3.7	42.2 × 10^3	3.31 ± 0.14	7.5 ± 0.1	2.3 × 10^3	5.5
Glc-1,6-BP	0.19 ± 0.04	415 ± 30.6	3038.9 × 10^3	0.09 ± 0.02	14.4 ± 0.7	158.1 × 10^3	5.2
Frc-1,6-BP	26.86 ± 3.35	218 ± 21.3	8.1 × 10^3	0.03 ± 0.01	3.6 ± 0.2	117.5 × 10^3	1,450

[a] K_m and K_{cat} values are means of triplicates with ± SD. Catalytic efficiency ratio is given in percentage and was calculated by the ratio of K_{cat}/K_m of Slr1334 and Sll0726.

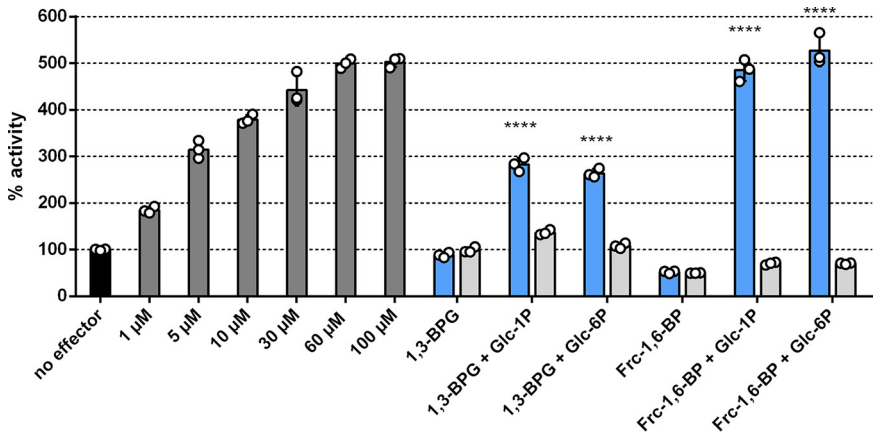

FIG 3 Activation of Sll0726 PGM reaction by Glc-1,6-BP or by the reaction products of Slr1334. Shown is the Sll0726 PGM activity in the presence of different effectors relative to the activity in the absence of effector molecules (set as 100%, black bar). The different bars represent the following reactions: Dark gray bars: Relative PGM activity in the presence of different concentrations of activator molecule Glc-1,6-BP, as indicated. Blue bars: Relative PGM activity in the presence of the supernatant of the Slr1334 reaction carried out with different combinations of substrates, as indicated. Light gray bars: Same conditions as adjacent blue bars, except that Slr1334 was replaced by Sll0726, as a control. Three biological replicates were measured for each datapoint. Error bars represent the SD; asterisks represent the statistical significance in comparison to the reaction without effectors.

reaction produced an estimated 30–60 μM the activating compound Glc-1,6-BP (Fig. 3). This implies that Frc-1,6-BP as phosphorylating sugar is about 10-fold more effective than 1,3-BPG for the Slr1334 reaction.

The product of the Slr1334 reaction is not degradable by the Frc-1,6-BP-aldolase. To confirm that the activating compound formed from Glc-1P/Glc-6P and Frc-1,6-BP through the Slr1334 reaction is in fact Glc-1,6-BP, we analyzed the reaction product via liquid chromatography-mass spectrometry (LC/MS). Therefore, we incubated Slr1334 together with 500 μM Frc-1,6-BP and 1 mM Glc-1P for 1.5 h. As a control, the same substrates were incubated without enzyme. Since LC/MS analysis does not allow discriminating Glc-1,6-BP from Frc-1,6-BP, we performed an additional reaction step to specifically degrade Frc-1,6-BP. Therefore, after heat inactivation, the reaction mixture was incubated with Frc-1,6-BP-aldolase (Fba) and glycerol-3-phosphate-dehydrogenase (GPDH) as well as 1 mM NADH:Fba specifically cleaves Frc-1,6-BP into dihydroxyacetone phosphate (DHAP) and glyceraldehyde-3P while Glc-1,6-BP is unaffected. GPDH subsequently forms glycerol-3-phosphate (glycerol-3P) and NAD^+ out of DHAP and NADH. This is necessary to enable full degradation of Frc-1,6-BP.

After this treatment, LC/MS analysis revealed that a compound with a mass corresponding to either Glc-1,6-BP or Frc-1,6-BP was present in the Slr1334 reaction while this mass was not detectable in the control reaction where no Slr1334 was present (Fig. 4). This indicates that Frc-1,6-BP in the control reaction was completely degraded in the subsequent reaction by Fba as expected, while Frc-1,6-BP in the Slr1334 reaction was metabolized into a molecule of the same mass that was not degraded by Fba. This is precisely what is expected when Glc-1,6-BP is produced from Frc-1,6-BP turn-over. Furthermore, the reaction products from the coupled GPDH reaction, NAD^+ and glycerol-3P were more abundant in the control reaction without Slr1334 compared to the reaction with Slr1334. This indicated that more Frc-1,6-BP was degraded out of the control reaction than out of the reaction containing Slr1334 due to partial conversion of Frc-1,6-BP into Glc-1,6-BP by Slr1334 (Fig. 4). Altogether, this experiment strongly indicated that in the presence of Slr1334, Frc-1,6-BP was partially utilized to form Glc-1,6-BP. The fact that only a part of Frc-1,6-BP was consumed could be either due to a too short reaction time or because the reaction reached an equilibrium state.

Slr1334 keeps Frc-1,6-BP and Glc-1,6-BP in an equilibrium. For investigating whether the formation of Glc-1,6-BP out of Glc-1P/Glc-6P and Frc-1,6-BP is an equilibrium reaction, we performed an enzymatic assay to determine the amount of the

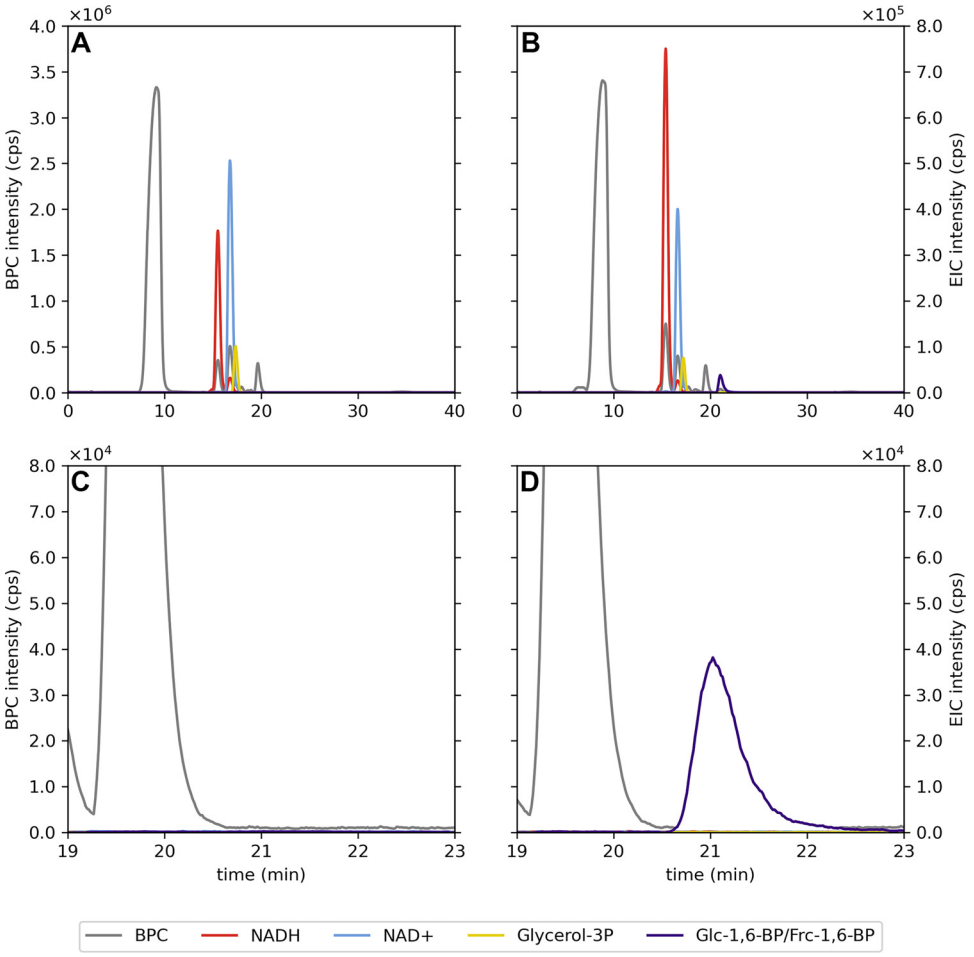

FIG 4 LC-MS analysis reveals that Slr1334 metabolizes Frc-1,6-BP into a molecule of identical mass that is not degraded by Frc-1,6-BP-aldolase. Analysis of the products of the reaction without (A) and with Slr1334 (B) via LC/MS. Shown are the base peak chromatograms (BPC) in the mass range (M-H)- *m/z* = 79–1,601 (gray) and the extracted ion chromatograms (EIC) based on the exact masses of NAD^+ $(M\text{-}H)^-$ = 662.101 *m/z* (light blue), NADH $(M\text{-}H)^-$ = 664.117 *m/z* (red), Glycerol 3-P $(M\text{-}H)^-$ = 171.006 *m/z* (yellow), Glc-1,6-BP/Frc-1,6-BP $(M\text{-}H)^-$ = 338.988 *m/z* (purple). The presence of the NAD^+ (blue) and Glycerol-3P (yellow) peaks in (B) shows that Frc-1,6-BP was not fully metabolized into Glc-1,6-BP. Magnification and adjustment of the graphs in (A) and (B) is clear evidence of the absence (C) or formation (D) of Glc-1,6-BP.

remaining Frc-1,6-BP. Therefore, Slr1334 was incubated with 500 μM Frc-1,6-BP and 1 mM Glc-1P for 1.5 h. As controls, the same assays were performed with Sll0726 or without any enzyme. After the reaction was stopped by heat inactivation, the supernatant was used to run the coupled Fba/GPDH assay in a dilution of 1:10, which would correspond to a final concentration of 50 μM Frc-1,6-BP if no Frc-1,6-BP was consumed. As further controls, standards of 50 μM and 25 μM Frc-1,6-BP were used in the Fba/GPDH assay. This experiment showed that the concentration of Frc-1,6-BP decreased by about 50% when in the first reaction Slr1334 was present, while apparently no Frc-1,6-BP was utilized in the control reactions (Fig. 5). This result agreed with the assumption that the reaction reaches an equilibrium at 50% product formation, either because of the reversibility of the reaction or product inhibition.

The Slr1334 reaction is reversible. To reveal whether Slr1334 can catalyze the proposed reverse reaction and synthesize Frc-1,6-BP from Glc-1,6-BP and fructose-1P (Frc-1P)/fructose-6P (Frc-6P), formation of Frc-1,6-BP was coupled to the Fba and GPDH reaction. For the assay, 50 μM Glc-1,6-BP was used and the reaction was started by the addition of 5 mM Frc-6-P. As control reaction, *Synechocystis* Sll0726 was used. In addition, we also tested PGM1 from rabbit since this type of PGM was stated to possibly catalyze this reaction albeit at a very low efficiency (22, 23). The results clearly showed

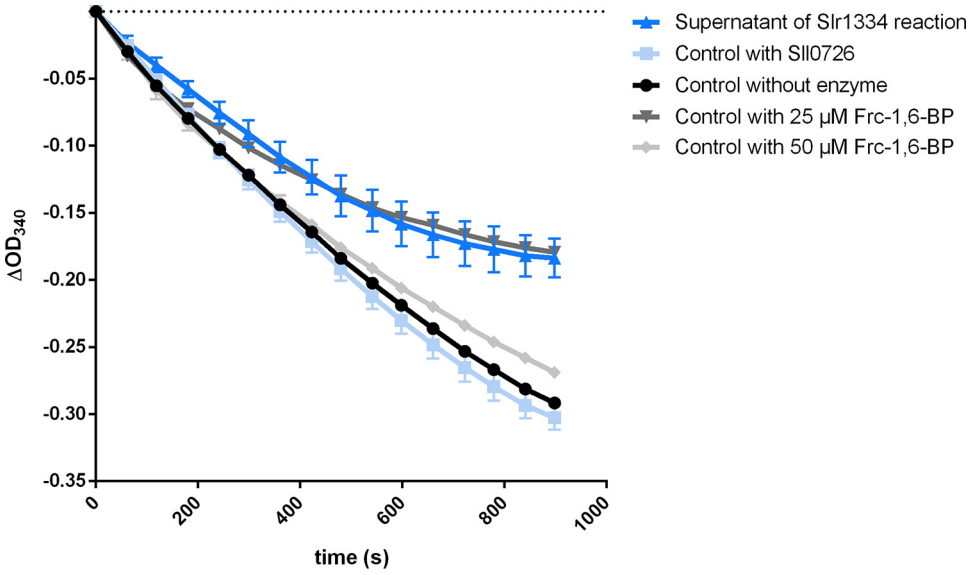

FIG 5 Slr1334 produces Glc-1,6-BP out of Frc-1,6-BP in an equilibrium reaction. Shown is the Frc-1,6-BP-aldolase activity: in dark blue, after addition of the supernatant of the Slr1334 reaction; in light blue, after addition of the supernatant of the Sll0726 reaction as a control; in black, after addition of the supernatant without any enzyme. In dark gray and light gray, the aldolase activity measured at Frc-1,6-BP concentrations of 25 μM and 50 μM, respectively, as further control. Frc-1,6-BP was used at concentrations of 500 μM in the Slr1334 reaction and respective control reactions. Therefore, its final concentration in the Sll0726 assay after 1:10 dilution was expected to be 50 μM assuming no consumption of Frc-1,6-BP in the Slr1334 reaction. Three replicates were measured for each datapoint. Error bars represent the SD.

that Slr1334 could produce Frc-1,6-BP, resulting in measurable aldolase activity while the Sll0726 and rabbit PGM controls showed no marked activity (Fig. 6a). Using this assay, we tried to determine the kinetic constants for the two substrates Frc-6-P and Glc-1,6-BP. For Frc-6P, a K_m of 1 mM and a K_{cat} of 1.2 s^{-1} could be determined (Fig. 6b, Table 3). By contrast, the affinity of Slr1334 for Glc-1,6-BP was so high that, even at the lowest measurable substrate concentrations (2 μM), the reaction proceeded with maximal velocity (Fig. 6c). Altogether these experiments unequivocally demonstrate that Slr1334 is the first characterized bacterial Glc-1,6-BP synthase. In contrast to the eukaryotic Glc-1,6-BP synthase, the prokaryotic enzyme uses Frc-1,6-BP as major phosphoryl donor for Glc-1,6-BP production.

The Glc-1,6-BP synthase reaction is also performed by other members of the cd05800 group. To determine whether the reaction catalyzed by Slr1334 is representative for αPHM enzymes of the cd05800 family, we decided to analyze the corresponding homologue from the human microbiome associated bacterium *Bacteroides salyersiae*. Therefore, we tested formation of Glc-1,6-BP under the same conditions as described above for Slr1334 by incubating the recombinant cd05800 enzyme from *B. salyersiae* with Frc-1,6-BP and Glc-1P or Glc-6P and subsequently adding the supernatant of this reaction to the Sll0726 assay. As a positive control we used the reaction of Slr1334.

The addition of the supernatant from the *B. salyersiae* cd05800 PGM increased the velocity of Sll0726 in a comparable manner as the supernatant of the Slr1334 reaction (Fig. 7). This indicates that similar amounts of Glc-1,6-BP have been formed in both reactions, hence revealing that *B. salyersiae* cd05800 PGM catalyzes the same reaction as Slr1334.

DISCUSSION

Among the key reactions in carbon metabolism are the phosphoryl transfer reactions on different phosphosugars, which are catalyzed by the members of the αPHM superfamily. These reactions are essential for glycogen metabolism, amino sugar metabolism as well as cell wall synthesis and are conserved throughout all domains of life. The interconversion of Glc-1P to Glc-6P and vice versa by PGM is by far the best

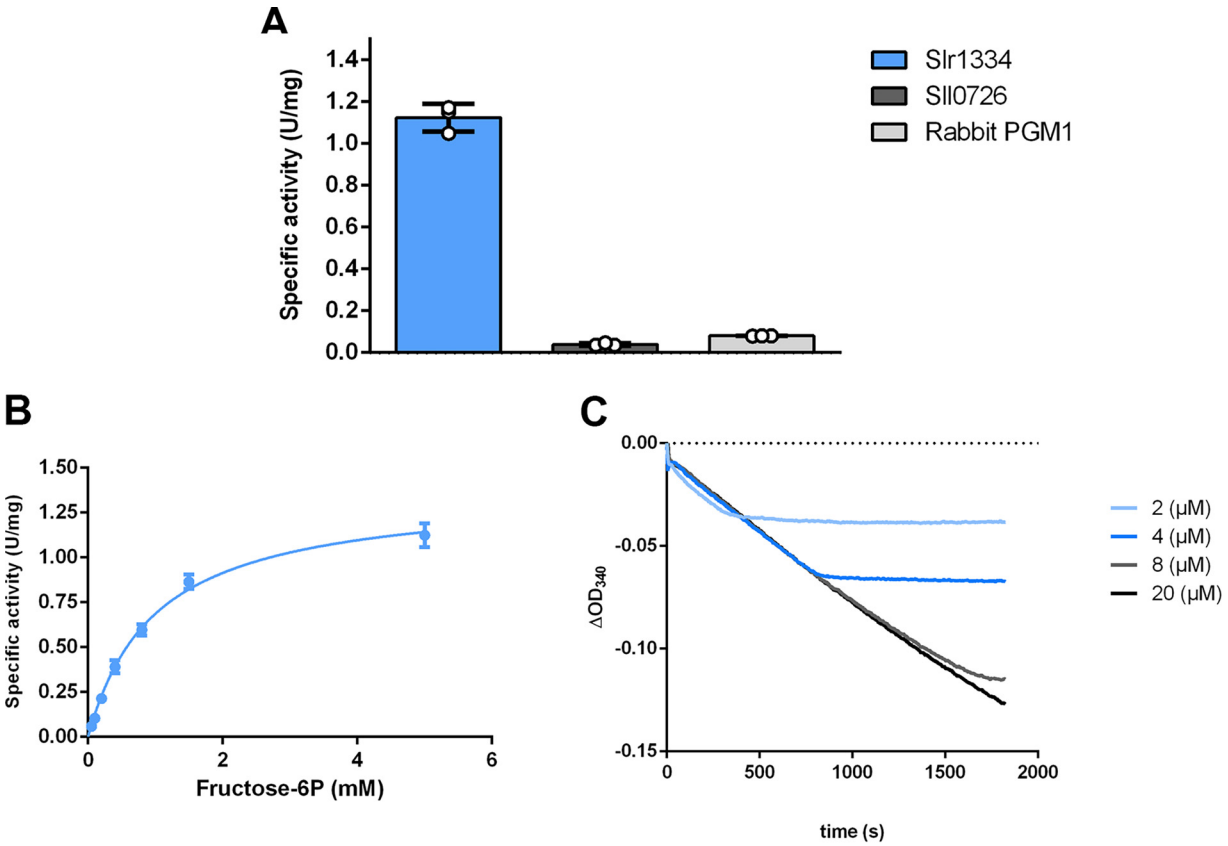

FIG 6 Slr1334 catalyzes the reverse reaction to form Frc-1,6-BP out of Glc-1,6-BP and Frc-6P. (A) Activity of Slr1334 (blue), Sll0726 (gray), and rabbit PGM1 (black) using 50 μM Glc-1,6-BP and 5 mM Frc-6P. (B) Michaelis-Menten kinetics of Slr1334 using different concentrations of Frc-6P and 50 μM Glc-1,6-BP. (C) Slr1334 reaction at different concentrations of Glc-1,6-BP and 0.5 mM Frc-6P. Three replicates were measured for each datapoint. Error bars represent the SD; asterisks represent the statistical significance.

studied of these reactions and investigation of PGM goes back to the 1940s. It has long been known that PGM requires Glc-1,6-BP as a activator (10). While in mammals free Glc-1,6-BP has been shown to derive from the reaction of the PGM2L1 enzyme utilizing Glc-1P and 1,3-BPG as substrates, its origin in prokaryotes has remained unknown (3).

In this study, we used the unicellular cyanobacterium *Synechocystis* sp. PCC6803 as a model organism to identify the first bacterial glucose-1,6-BP synthase. This reversible reaction is a novel function of a member of a distinct αPHM subfamily producing free α-d-Glc-1,6-BP and Frc-6P from Frc-1,6-BP and Glc-1P/Glc-6P.

Glc-1,6-BP is essential for PGM activity due to the requirement for phosphorylation of the serine residue at the active site for enzyme activation. The activating reaction converts Glc-1,6-BP into either Glc-1P or Glc-6P. After this initial activation, the interconversion of Glc-1P to Glc-6P is mediated by a transfer of the phosphate group from the serine residue at the active site to the 1′ or 6′ position of the substrate respectively, forming a Glc-1,6-BP intermediate. This intermediate has to reconfigure inside the enzyme and transfer the phosphate of its 6′ or 1′ position back to the active site serine leading to the release of Glc-6P or Glc-1P, respectively. As a result of this mechanism, the active site remains phosphorylated, and the enzyme is ready for a new cycle. However, it has been shown that the phosphorylation of PGM at the active site is lost after an aver-

TABLE 3 Kinetic parameters of Frc-1,6-BP synthesis by Slr1334[a]

Substrate	K_m (mM)	K_{cat} (s^{-1})	K_{cat}/K_m ($M^{-1}s^{-1}$)
Glc-1,6-BP	$<$0.002	1.2 $\pm$ 0.03	600,000
Frc-6P	1.0 $\pm$ 0.07		$>$1,200

[a] K_m and Kcat values are means of triplicates with $\pm$ SD.

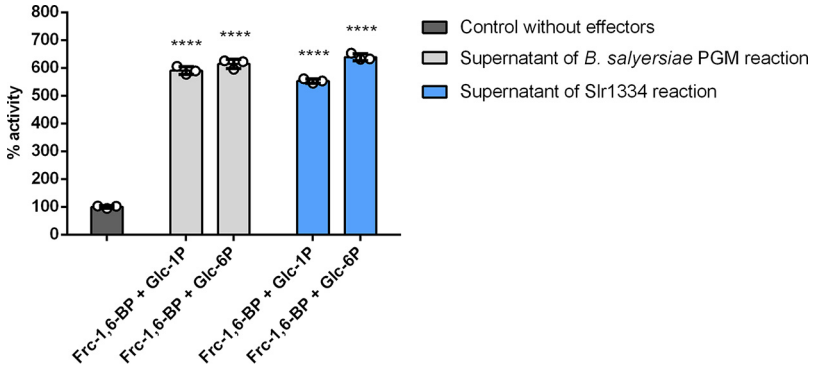

FIG 7 Slr1334 homologue from *B.salyersiae* also forms Glc-1,6-BP out of Frc-1,6-BP. Shown is the Sll0726 PGM activity in the presence of different effectors relative to the activity in the absence of effector molecules (set as 100%, dark gray bar): The different bars represent the following reactions: Light gray bars: Relative PGM activity in the presence of the supernatant of the *B. salyersiae* PGM reaction carried out with different combinations of substrates, as indicated. Blue bars: Same conditions as adjacent blue bars, except that *B. salyersiae* PGM was replaced by Slr1334, as a positive control. Error bars represent the SD; asterisks represent the statistical significance in comparison to the reaction without effectors.

age of 15–20 reaction cycles by a spontaneous dissociation of the intermediate Glc-1,6-BP leaving behind an inactive dephosphoenzyme. Therefore, a constant level of Glc-1,6-BP is necessary to ensure that PGM is kept in an active state (24, 25). While the loss of the intermediate might be regarded as an unfavorable event, it can also be considered as a regulatory mechanism that enables regulation of PGM activity based on Glc-1,6-BP levels. For other αPHMs like PMM and PNGM it is known that the corresponding intermediates (e.g., α-d-mannose-1,6-BP and α-d-glucosamine-1,6-BP) are formed during the reaction of the respective enzymes in the same way as for PGM but no source of those intermediates is known that would enable an initial activation of these αPHMs or would keep them in an active state overtime when phosphorylation is lost. However, because many members of the αPHM family show at least some residual PGM activity, Glc-1,6-BP was suggested to be the activating compound for these enzymes as well. This has in fact been shown for PNGM from *E. coli* which is considered to be an essential enzyme (26). This makes the role of Glc-1,6-BP in carbon metabolism even more relevant and would explain the failed attempts to delete the *slr1334* gene (19).

In mammals, it was shown that Glc-1,6-BP can also regulate central enzymes of carbon pathways by inhibiting hexokinases, 6-phosphogluconate dehydrogenase and fructose-1,6-bisphosphatase and by activating phosphofructokinase and pyruvate kinase (12). Further studies in mammals showed that Glc-1,6-BP is especially elevated in brain tissue to a level that highly exceeds the regulatory concentrations needed for PGM activity, and that reduced levels of Glc-1,6-BP cause severe neurological problems (27). This indicates that at least in mammals there are likely more functions of Glc-1,6-BP to be discovered. Given the important role of Glc-1,6-BP in eukaryotic metabolism, it is surprising that very little is known on the role of Glc-1,6-BP in bacterial physiology. The only study about the origin of α-d-Glc-1,6-BP production in bacteria proposed a phosphodismutase reaction with Glc-1P as the sole substrate in *E. coli* (28). Moreover, the levels of Glc-1,6-BP in eukaryotes are affected by a specific Glc-1,6-BP phosphatase, PMM1, which is a phosphomannomutase that is not part of the αPHM superfamily. Whether a homologue exists in bacteria is currently unknown (29).

In the absence of Glc-1,6-BP, both Slr1334 and Sll0726 showed low PGM activity. This residual activity can be explained by the fact that a phosphorylation of the active site serine can also be achieved at high concentrations of Glc-1P but at a much lower efficiency, leading to high K_m values and overall strongly reduced activity (11). In the presence of Frc-1,6-BP, Sll0726 was strongly inhibited, which agrees with the inhibitory effect of Frc-1,6-BP on other PGMs (20, 21). By contrast, Frc-1,6-BP enhanced the overall

catalytic activity of Slr1334, primarily because of a strongly decreased K_m. This effect can now be attributed to the formation of the activator Glc-1,6-BP.

Like mammalian PGM2L1, Slr1334 can utilize 1,3-BPG as a phosphorylating compound for Glc-1,6-BP formation, however with a much lower efficiency than Frc-1,6-BP. Although it cannot be excluded that 1,3-BPG could play a role under certain conditions, Frc-1,6-BP seems to be more important as it can accumulate to high levels in bacteria (30).

For the mammalian PGM2L1 a reverse reaction (formation of 1,3-BPG and Glc-1P from Glc-1,6-BP and 3-PG) has not been shown. For Slr1334, we could clearly show reversibility of the reaction, producing Frc-1,6-BP from Glc-1,6-BP and Frc-6P. Provided that both directions of the reaction have similar kinetic properties, Slr1334 appears to be a *bona-fide* Glc-1,6-BP synthase, which is prone to activate the main PGM Sll0726.

In contrast to Glc-1,6-BP, Frc-1,6-BP is an obligatory intermediate in glycolysis, gluconeogenesis and Calvin-Benson-Bassham cycle. In contrast to mammalian PGM2L1, *Synechocystis* Slr1334 uses this sugar as the major substrate for Glc-1,6-BP synthesis. This links the synthesis of Glc-1,6-BP to the levels of Frc-1,6-BP. Its steady state level depends on the activity of the opposing reactions of phosphofructokinase (Pfk) and fructose-1,6-bisphosphatase (FBPase), both of which are regulated in an opposite manner: While PFK is usually activated by the low energy state metabolites ADP and AMP and downregulated by the high energy state metabolites ATP and citrate, FBPase is downregulated by AMP while unaffected by high energy compounds. The level of Frc-1,6-BP is further determined by the Frc-1,6-BP-aldolase activity. Frc-1,6-BP is also known to be an allosteric activator of pyruvate kinase (PK), the final step in glycolysis (31).

Altogether, in the cyanobacterium *Synechocystis* PCC6803, Frc-1,6-BP appears to have two counteracting effects on PGM activity. On the one hand, it acts as a direct inhibitor of PGM; on the other hand, it gives rise to the synthesis of the PGM activator Glc-1,6-BP through the activity of Slr1334. Furthermore, since these double phosphorylated sugars may affect further enzyme reactions, by connecting these two metabolites, Slr1334 might represent a crucial regulatory point in glycolysis (Fig. 8). This conclusion would further underline the essential role of *slr1334* (19).

Interestingly, our phylogenetic analysis revealed the cd05800 subfamily as the most primordial group of phosphoglucomutases. This group appears to be especially present in bacterial classes that are considered deeply branching bacteria meaning they are relatively close to the last common universal ancestor. Examples for this are the classes of Deinococci, Aquificae, Thermotogae, Bacteroidetes, and Cyanobacteria, where this PGM subfamily is widely distributed. This finding is supported by the fact that cd05800 members can also be found in archaea. In agreement with this, the first characterized representative of this group, Slr1334 shows both PGM and Glc-1,6-BP activity. This suggests that in primordial systems these PGMs with broad functionality could have performed PGM reactions without the requirement for specific Glc-1,6-BP synthase enzymes. During subsequent functional diversification, the PGMs may have adopted unique functions, with specialization toward efficient conversion of Glc-6-P into Glc-1P on the one hand. On the other hand, they may have lost the ability to sufficiently catalyze other reactions like Glc-1,6-BP synthesis. This assumption agrees with our observation that in some bacteria the primordial, more universal cd05800 PGM is the only subfamily found. In contrast, the more specialized and highly efficient cd03085 and cd05801 PGMs are always accompanied by other subfamily members (mainly cd05800). Conversely, the cd03089 PGM/PMM, often associated with pathogenic bacteria, is never accompanied with a cd05800 representative which raises the question how those strains produce Glc-1,6-BP (Table S2). To clarify these issues, further investigations on αPHM members from various bacterial groups are required.

We were able to show that the cd05800 PGM from the human gut commensal bacterium *B. salyersiae* also catalyzes the synthesis of Glc-1,6-BP out of Frc-1,6-BP like Slr1334 (Fig. 7). In the case of *B. salyersiae*, the enzyme appears to have an even higher catalytic efficiency for the Glc-1,6-BP synthase reaction than for the standard PGM reaction (Fig. S1 in the supplemental material). Therefore, we conclude that the formation

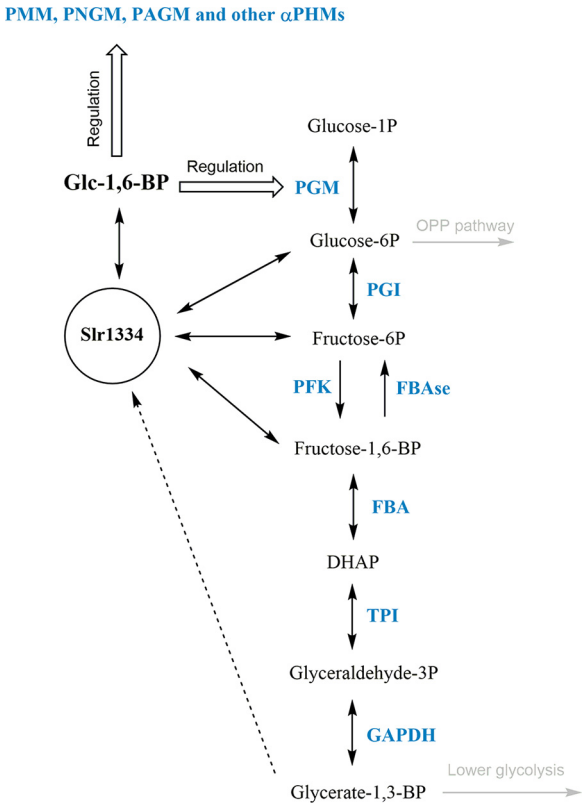

FIG 8 Potential role of Slr1334 in glycolysis. Shown is the potential role of Slr1334 in regulating activity of αPHMs and the concentration of key metabolites in glycolysis. PGM: Phosphoglucomutase; PGI: Glc-6P-Isomerase; PFK: Phosphofruktokinase; FBAse: fructose-6P phosphatase; FBA: Frc-1,6-BP-aldolase; TPI: Triosephosphate isomerase; GAPDH: Glyceraldehyde-3P dehydrogenase; DHAP: Dihydroxyacetone phosphate.

of Glc-1,6-BP might be a general feature of this PHM subfamily. However, further studies on members of this group are required to support this hypothesis.

Interestingly, members of the cd05800 group are also present in emerging human pathogenic species like *Vibrio*, *Eggerthella*, and *Brachyospyra* (Fig. 1) and are likely to play a key role in the metabolism of these pathogens. In fact, due to their crucial role in capsule and cell wall synthesis PGMs have been suggested as novel targets for the development of anti-infectives in prophylactic and therapeutic interventions (5, 32). It is tempting to speculate that Glc-1,6-BP synthases of the cd05800 family, in virtue of their absence in eukaryotes, may also be interesting candidates for the development of novel drugs modulating the microbiota with little collateral damage to the host.

MATERIALS AND METHODS

Isothermal, single-reaction DNA assembly (Gibson cloning). Cloning was performed as described by Gibson, Young (33) using *E. coli* NEB10β cells (details in Table S5). All primers and plasmids used are shown in Table S3 and Table S4 in the supplemental material, respectively.

Cultivation of *Escherichia coli*. If not otherwise stated *E. coli* was grown in Luria-Bertani medium at 37°C (34). For growth on plates, 1.5% (wt/vol) agar-agar was added. For cells containing plasmids, the appropriate concentration of antibiotics was used. All *E. coli* strains used in this study are listed in Table S5 in the supplemental material.

Protein overexpression and purification. The plasmids used for protein overexpression are shown in Table S4 in the supplemental material. *Escherichia coli* Rosetta-gami (DE3) (details Table S5) was used for the overexpression of all proteins. For this, cells were cultivated in 2xYT (3.5% tryptone, 2% yeast extract, 0.5% NaCl; 1L of culture in 5L flasks) at 37°C until reaching exponential growth (OD_{600} 0.6–0.8). Protein overexpression was induced by adding 75 μg/L anhydrotetracycline, followed by incubation at 20°C for 16 h. Cells were harvested by centrifugation at 4000 g for 10 min at 4°C. Cell disruption was performed by sonication in 40 mL of lysis buffer (100 mM Tris-HCl pH 7.5, 500 mM NaCl, 10 mM $MgCl_2$, 20 mM Imidazole for His-tagged proteins and 100 mM Tris-HCl pH 8, 150 mM NaCl, 10 mM $MgCl_2$ for Strep-tagged proteins); lysis buffers were supplemented with DNase I and cOmplete^{TM} protease inhibitor cocktail (Roche, Basel).

The cell lysate was centrifuged at 40,000 g for 45 min at 4°C and the supernatant was filtered with a 0.22 μM filter.

For the purification of His-tagged proteins, 5 mL Ni-NTA HisTrap columns (GE Healthcare, IL, USA) were used. The cell extracts were loaded onto the columns, washed with wash buffer (50 mM Tris-HCl pH 7.4, 500 mM NaCl, and 50 mM Imidazole) and eluted with elution buffer (50 mM Tris-HCl pH 7.4, 500 mm NaCl, and 500 mM Imidazole).

Measurement of PGM activity of Sll0726 and Slr1334 *in vitro*. Buffer for enzymatic reactions was composed of 50 mM HEPES-KOH pH 7.5, 150 mM KCl, 10 mM $MgCl_2$, 1 mM $NADP^+$, 1 mM DTT, and 1 U/mL G6PDH from *Saccharomyces cerevisiae* (G6378, Sigma-Aldrich). For Sll0726 activity, 60 ng of Strep-tagged purified protein was added to each reaction. For slr1334 activity, 650 ng of purified protein was added. For tests with saturating Glc-1,6-BP concentrations, 60 μM Glc-1,6-BP have been used. Reaction was started by the addition of glucose-1P. Reactions were carried out in a total of 300 μL in a 96-well microplate. Absorption change at 340 nm was continuously measured for 15 min at 30°C in a TECAN Spark Multiplate reader (Tecan Group AG, Männedorf, Switzerland). At least three replicates were measured.

Measurement of Glc-1,6-BP formation. The reaction buffer was composed of 50 mM HEPES-KOH pH 7.5, 150 mM KCl and 10 mM $MgCl_2$. To test the formation of Glc-1,6-BP out of Frc-1,6-BP 1 mM Frc-1,6-BP, 1 mM Glc1P or 1 mM Glc-6P were added in different combinations. To test the formation of Glc-1,6-BP out of 1,3-BPG instead of Frc-1,6-BP, 1 mM ATP, 1 mM 3-PG and 60 μg PGK have been used. Sll0726 and Slr1334 concentration were 30 μg/mL. The reactions were performed for 1.5 h at 30°C followed by heat inactivation at 90°C for 10 min with subsequent centrifugation at 25000 g for 10 min at 4° C. The supernatants of the various reactions were used at 1:10 dilution in the Sll0726 activity assay.

Measurement of Frc16BP formation by coupling to Frc-1,6-BP aldolase assay. To measure the formation of Frc-1,6-BP by Slr1334, the reaction buffer was composed of 50 mM HEPES-KOH pH 7.5, 150 mM KCl, 10 mM $MgCl_2$, 0.2 mM NAD, 7 μg Slr1334, 1U/mL FBP-aldolase from rabbit muscle and 1U/mL GDH from rabbit muscle. Concentrations of Glc-1,6-BP and Frc-6P were varying depending on the experiment. Reaction was started by the addition of Glc-1,6-BP or Frc-6P depending on the experiment.

To measure residual Frc-1,6-BP after running the Slr1334 reaction, the buffer was composed of 50 mM HEPES-KOH pH 7.5, 150 mM KCl, 10 mM $MgCl_2$, 0.2 mM NAD, 0.02U/mL aldolase from rabbit muscle and 1U/mL GDH from rabbit muscle.

All reactions were carried out in a total of 300 μL in a 96-well microplate. Absorption change at 340 nm was continuously measured for 15 min at 30°C in a TECAN Spark Multiplate reader (Tecan Group AG, Männedorf, Switzerland). The enzymatic activity was then calculated. At least three replicates were measured.

LC-MS measurement. *Sample preparation*. Reaction buffer was composed of 50 mM HEPES-KOH pH 7.5, 150 mM KCl and 10 mM $MgCl_2$. For the reaction without enzyme 500 μM Frc-1,6-BP and 1 mM Glc1-P were added. For the Slr1334 reaction, 30 μg of Slr1334 have been used additionally. Reaction was carried out in a total volume of 1 mL at 30°C for 1h. Afterwards, reaction was stopped by heat inactivation at 90° C followed by centrifugation at 25000 g for 10 min at 4°C.

For degradation of Frc-1,6-BP, 1 mM NADH, 2U/mL of aldolase from rabbit muscle and 2U/mL of GDH from rabbit muscle were added. Reaction was carried out followed by inactivation at the same conditions as before.

***LC/MS analysis*.** LC/MS analysis was performed using an electrospray ionization time of flight (ESI-TOF) mass spectrometer (MicrOTOF II; Bruker Daltonics), operated in negative ion-mode connected to an UltiMate 3000 high-performance liquid chromatography (HPLC) system (Dionex). The separation in the HPLC was carried out using a SeQuant ZIC-pHILIC column (PEEK 150 $\times$ 2.1 mm, 5 μm, 110 Å, Merck) at 30°C with an CH_3CN (buffer A) and 100 mM $(NH_4)_2CO_3$, pH 9 (buffer B) buffer system. A single run (injection volume of 5 μL) was performed with a flow rate of 0.2 mL/min and a linear gradient of 25 min, reducing the concentration of buffer A from 82% to 42%. Before (5 min) and after (10 min) the gradient, the column was equilibrated with 82% buffer A.

Phylogenetic analysis of αPHM subfamilies. The occurrence of members of the αPHM subfamilies was investigated in organisms included in the NCBI RefSeq_protein database using the default settings of blastp. The search returned 2140 hits for Slr1334 homologues and >5000 hits for Sll0726 homologues by using the following threshold:

E-value $\leq 10^{-40}$; sequence identity $\geq$ 30%; Query coverage $\geq$ 95%

Phylogenetic tree data were created using the ClustalW implementation from the European Bioinformatics Institute and the phylogenetic tree was created using the Interactive Tree of Life (iTOL) v5 online tool (35, 36).

Statistical analysis. Statistical details for each experiment can be found in the figure legends. GraphPad PRISM was used to perform one-sided ANOVA to determine the statistical significance. Asterisks (*) in the figures symbolize the *P*-value: one asterisk represents $P \leq 0.05$, two asterisks $P \leq 0.01$, three asterisks $P \leq 0.001$, and four asterisks $P \leq 0.0001$.

SUPPLEMENTAL MATERIAL

Supplemental material is available online only.

FIG S1, TIF file, 0.1 MB.

TABLE S1, DOCX file, 0.02 MB.

TABLE S2, DOCX file, 0.02 MB.

TABLE S3, DOCX file, 0.01 MB.

TABLE S4, DOCX file, 0.01 MB.
TABLE S5, DOCX file, 0.02 MB.

ACKNOWLEDGMENTS

We thank Libera Lo Presti for her assistance in writing this manuscript and Gaia Bianchi for support in performing enzymatic assays.

This work was supported by FOR2816 "The Autotrophy-Heterotrophy Switch in Cyanobacteria: Coherent Decision-Making at Multiple Regulatory Layers" and EXC2121 "Controlling Microbes to Fight Infections" (CMFI).

N.N. performed cloning, protein purification, enzymatic assays phylogenetic analysis and wrote manuscript. S.F. performed LC/MS analysis. K.F. conceived study, interpreted data, and edited manuscript.

We declare no competing interest.

REFERENCES

1. Shackelford GS, Regni CA, Beamer LJ. 2004. Evolutionary trace analysis of the α-D-phosphohexomutase superfamily. Protein Sci 13:2130–2138. https://doi.org/10.1110/ps.04801104.
2. Stiers KM, Muenks AG, Beamer LJ. 2017. Biology, mechanism, and structure of enzymes in the α-d-phosphohexomutase superfamily. Adv Protein Chem Struct Biol 109:265–304. https://doi.org/10.1016/bs.apcsb.2017.04.005.
3. Maliekal P, Sokolova T, Vertommen D, Veiga-da-Cunha M, Van Schaftingen E. 2007. Molecular identification of mammalian phosphopentomutase and glucose-1,6-bisphosphate synthase, two members of the alpha-D-phosphohexomutase family. J Biol Chem 282:31844–31851. https://doi.org/10.1074/jbc.M706818200.
4. Lu S, Wang J, Chitsaz F, Derbyshire MK, Geer RC, Gonzales NR, Gwadz M, Hurwitz DI, Marchler GH, Song JS, Thanki N, Yamashita RA, Yang M, Zhang D, Zheng C, Lanczycki CJ, Marchler-Bauer A. 2020. CDD/SPARCLE: the conserved domain database in 2020. Nucleic Acids Res 48:D265–D268. https://doi.org/10.1093/nar/gkz991.
5. Regni C, Tipton PA, Beamer LJ. 2002. Crystal structure of PMM/PGM: an enzyme in the biosynthetic pathway of P aeruginosa virulence factors. Structure 10:269–279. https://doi.org/10.1016/S0969-2126(02)00705-0.
6. Regni C, Naught L, Tipton PA, Beamer LJ. 2004. Structural basis of diverse substrate recognition by the enzyme PMM/PGM from P aeruginosa. Structure 12:55–63. https://doi.org/10.1016/j.str.2003.11.015.
7. Akutsu J-I, Zhang Z, Tsujimura M, Sasaki M, Yohda M, Kawarabayasi Y. 2005. Characterization of a thermostable enzyme with phosphomannomutase/phosphoglucomutase activities from the hyperthermophilic archaeon pyrococcus horikoshii OT3. J Biochem 138:159–166. https://doi.org/10.1093/jb/mvi115.
8. Liu Y, Ray WJ, Jr, Baranidharan S. 1997. Structure of rabbit muscle phosphoglucomutase refined at 2.4 A resolution. Acta Crystallogr D Biol Crystallogr 53:392–405. https://doi.org/10.1107/S0907444997000875.
9. Backe PH, Laerdahl JK, Kittelsen LS, Dalhus B, Mørkrid L, Bjørås M. 2020. Structural basis for substrate and product recognition in human phosphoglucomutase-1 (PGM1) isoform 2, a member of the α-d-phosphohexomutase superfamily. Sci Rep 10:5656. https://doi.org/10.1038/s41598-020-62548-0.
10. Leloir LF, Trucco RE, Cardini CE, Paladini AC, Caputto R. 1948. The co-enzyme of phosphoglucomutase. Arch Biochem 19:339.
11. Naught LE, Tipton PA. 2001. Kinetic mechanism and pH dependence of the kinetic parameters of Pseudomonas aeruginosa phosphomannomutase/phosphoglucomutase. Arch Biochem Biophys 396:111–118. https://doi.org/10.1006/abbi.2001.2618.
12. Carreras J, Bartrons R, Climent F, Cusso R. 1986. Bisphosphorylated metabolites of glycerate, glucose, and fructose: functions, metabolism and molecular pathology. Clinical Biochemistry 19:348–358. https://doi.org/10.1016/S0009-9120(86)80008-X.
13. Joshi JG, Handler P. 1964. Phosphoglucomutase: I. Purification and properties of phosphoglucomutase from *escherichia coli*. J Biol Chem 239:2741–2751. https://doi.org/10.1016/S0021-9258(18)93809-3.
14. Morán-Zorzano MT, Viale AM, Muñoz FJ, Alonso-Casajús N, Eydallín GG, Zugasti B, Baroja-Fernández E, Pozueta-Romero J. 2007. *Escherichia coli* AspP activity is enhanced by macromolecular crowding and by both glucose-1,6-bisphosphate and nucleotide-sugars. FEBS Lett 581:1035–1040. https://doi.org/10.1016/j.febslet.2007.02.004.
15. Spat P, Klotz A, Rexroth S, Macek B, Forchhammer K. 2018. Chlorosis as a developmental program in cyanobacteria: the proteomic fundament for survival and awakening. Molecular & Cellular Proteomics 17(9):1650–1669. https://doi.org/10.1074/mcp.RA118.000699.
16. Lindahl M, Florencio FJ. 2003. Thioredoxin-linked processes in cyanobacteria are as numerous as in chloroplasts, but targets are different. Proc Natl Acad Sci U S A 100:16107–16112. https://doi.org/10.1073/pnas.2534397100.
17. Mehra-Chaudhary R, Mick J, Tanner JJ, Henzl MT, Beamer LJ. 2011. Crystal structure of a bacterial phosphoglucomutase, an enzyme involved in the virulence of multiple human pathogens. Proteins 79:1215–1229. https://doi.org/10.1002/prot.22957.
18. Doello S, Neumann N, Forchhammer K. 2022. Regulatory phosphorylation event of phosphoglucomutase 1 tunes its activity to regulate glycogen metabolism. FEBS J. https://doi.org/10.1111/febs.16471.
19. Liu L, Hu HHua, Gao H, Xu X. 2013. Role of two phosphohexomutase genes in glycogen synthesis in *Synechocystis sp.* PCC6803. Chin Sci Bull 58:4616–4621. https://doi.org/10.1007/s11434-013-5958-0.
20. Maino VC, Young FE. 1974. Regulation of glucosylation of teichoic acid: II. Partial characterization of phosphoglucomutase in bacillus subtilis 168. J Biol Chem 249:5176–5181. https://doi.org/10.1016/S0021-9258(19)42344-2.
21. Fazi A, Piacentini MP, Piatti E, Accorsi A. 1990. Purification and partial characterization of the phosphoglucomutase isozymes from human placenta. Prep Biochem 20:219–240. https://doi.org/10.1080/00327489008050198.
22. Passonneau JV, Lowry OH, Schulz DW, Brown JG. 1969. Glucose 1,6-diphosphate formation by phosphoglucomutase in mammalian tissues. J Biol Chem 244:902–909. https://doi.org/10.1016/S0021-9258(18)91871-5.
23. Hirose M, Ueda M, Chiba H. 1976. Multifunctional properties of beef liver phosphoglucomutase. Agricultural and Biological Chemistry 40:2433–2439. https://doi.org/10.1080/00021369.1976.10862415.
24. Naught LE, Tipton PA. 2005. Formation and reorientation of glucose 1,6-bisphosphate in the PMM/PGM reaction: transient-state kinetic studies. Biochemistry 44:6831–6836. https://doi.org/10.1021/bi0501380.
25. Ray WJ, Jr, Roscelli GA. 1964. A kinetic study of the phosphoglucomutase pathway. J Biol Chem 239:1228–1236. https://doi.org/10.1016/S0021-9258(18)91416-X.
26. Jolly L, Pompeo F, van Heijenoort J, Fassy F, Mengin-Lecreulx D. 2000. Autophosphorylation of phosphoglucosamine mutase from *Escherichia coli*. J Bacteriol 182:1280–1285. https://doi.org/10.1128/JB.182.5.1280-1285.2000.
27. Morava E, Schatz UA, Torring PM, Abbott M-A, Baumann M, Brasch-Andersen C, Chevalier N, Dunkhase-Heinl U, Fleger M, Haack TB, Nelson S, Potelle S, Radenkovic S, Bommer GT, Van Schaftingen E, Veiga-da-Cunha M. 2021. Impaired glucose-1,6-biphosphate production due to bi-allelic PGM2L1 mutations is associated with a neurodevelopmental disorder. Am J Hum Genet 108:1151–1160. https://doi.org/10.1016/j.ajhg.2021.04.017.
28. Leloir LF, Trucco RE. and., 1949. The formation of glucose diphosphate by Escherichia coli. Arch Biochem 24:65–74.
29. Veiga-da-Cunha M, Vleugels W, Maliekal P, Matthijs G, Van Schaftingen E. 2008. Mammalian phosphomannomutase PMM1 is the brain IMP-sensitive glucose-1,6-bisphosphatase. J Biol Chem 283:33988–33993. https://doi.org/10.1074/jbc.M805224200.

30. Bennett BD, Kimball EH, Gao M, Osterhout R, Van Dien SJ, Rabinowitz JD. 2009. Absolute metabolite concentrations and implied enzyme active site occupancy in *Escherichia coli*. Nat Chem Biol 5:593–599. https://doi.org/10.1038/nchembio.186.
31. Waygood EB, Mort JS, Sanwal BD. 1976. The control of pyruvate kinase of *Escherichia coli*. Binding of substrate and allosteric effectors to the enzyme activated by fructose 1,6-bisphosphate. Biochemistry 15:277–282. https://doi.org/10.1021/bi00647a006.
32. Zhang Y, Li T, Zhang J, Li Z, Zhang Y, Wang Z, Feng H, Wang Y, Chen C, Zhang H. 2016. The Brucella melitensis M5–90 phosphoglucomutase (PGM) mutant is attenuated and confers protection against wild-type challenge in BALB/c mice. World J Microbiol Biotechnol 32:58. https://doi.org/10.1007/s11274-016-2015-6.
33. Gibson DG, Young L, Chuang R-Y, Venter JC, Hutchison CA, Smith HO. 2009. Enzymatic assembly of DNA molecules up to several hundred kilobases. Nat Methods 6:343–345. https://doi.org/10.1038/nmeth.1318.
34. Bertani G. 1951. Studies on lysogenesis: I. The mode of phage liberation by lysogenic *Escherichia coli*. J Bacteriol 62:293–300. https://doi.org/10.1128/jb.62.3.293-300.1951.
35. Letunic I, Bork P. 2021. Interactive Tree of Life (iTOL) v5: an online tool for phylogenetic tree display and annotation. Nucleic Acids Res 49:W293–W296. https://doi.org/10.1093/nar/gkab301.
36. Madeira F, Park YM, Lee J, Buso N, Gur T, Madhusoodanan N, Basutkar P, Tivey ARN, Potter SC, Finn RD, Lopez R. 2019. The EMBL-EBI search and sequence analysis tools APIs in 2019. Nucleic Acids Res 47:W636–W641. https://doi.org/10.1093/nar/gkz268.